

# Context-Aided Inertial Navigation via Belief Condensation

Javier Prieto, *Member, IEEE*, Santiago Mazuelas, *Member, IEEE*, and Moe Z. Win, *Fellow, IEEE*

**Abstract**—Inertial navigation systems suffer from drift errors that degrade their performance. Main current techniques mitigate such errors by detecting stance phases under the specific context of pedestrian walking with a foot-mounted inertial measurement unit (IMU). Existing approaches achieve acceptable performances only in simple circumstances, such as smooth movements and short periods of time. In addition, they lack a principled unifying methodology to exploit contextual information. In this paper, we establish a general framework for context-aided inertial navigation, and present efficient algorithms for its implementation based on the inference technique called belief condensation (BC). The performance of the proposed techniques is evaluated against the state of the art through an experimental case study. Our results show that the proposed techniques can remarkably improve the navigation accuracy while keeping moderate complexities.

**Index Terms**—Inertial navigation, belief condensation, contextual information, context learning, pedestrian dead reckoning.

## I. INTRODUCTION

NETWORK NAVIGATION can enable critical applications including logistics, medical services, search and rescue operations, automotive safety, and military systems [1]–[5]. The performance of the global navigation satellite systems (GNSS) in open areas boosted the development of a wide range of location-based services [6] and currently there is an increasing interest for high-accuracy navigation in harsh propagation environments [7]–[14]. Techniques based on wireless networks can provide suitable performance under certain circumstances but become inefficient in situations where it is not desirable to rely on an infrastructure [15]–[18].

Inertial navigation is becoming an increasingly popular positioning paradigm, especially given the recent emergence of iner-

tial measurement units (IMUs) based on micro-electro-mechanical systems (MEMS). Inertial navigation systems determine the position and orientation of a mobile agent by integrating measurements from an IMU carried by the agent [19]–[31]. These systems do not require any infrastructure other than the IMU itself, which makes them a preferred option for navigation in many scenarios, e.g., blue-force tracking, search and rescue operations, and pedestrian guidance.

Inertial navigation systems collect measurements related to positions and orientations. In particular, most IMUs obtain force measurements and angular velocities from accelerometers and gyroscopes. IMU measurements are used to estimate the agent's position by means of its variation in time. Such position estimation is commonly addressed from a Bayesian perspective through filtering algorithms. These algorithms recursively estimate the current positional state from previous estimates and current measurements [20]–[31].

The performance of inertial navigation systems degrades due to the accumulation of positional errors in time, resulting in the so-called positional *drift* [21]. Since the IMU measurements are related to positions' time derivatives, the positional error inevitably increases with time. Conventional techniques can only offer acceptable performance for short time periods [19]–[24]. Even minuscule errors present in the measurements collected by high-performance IMUs based on fiber-optic-gyros (FOG) lead to growth in the position estimation error [32]. Therefore, finding a solution to the drift problem is crucial to the development of robust inertial navigation systems.

The drift problem can be mitigated by exploiting the agent's specific *context*. Most of existing approaches are limited to the context in which the agent is a pedestrian and the IMU is mounted on the foot. Under that context, small values of acceleration and angular velocity imply stance phases of walking (i.e., the foot is on the ground) and hence small values of velocity (i.e., the IMU is motionless). Currently, the constraints imposed by such a context are used by performing zero-velocity updates (ZUPTs) when stationary stance phases are detected. At each time step, this detection is accomplished either by using a window of both past and future inertial measurements [19]–[24] or by exploiting additional measurements obtained from radar or RF sensors [25], [26]. More recent works also exploit other contextual information besides pedestrian foot-mounted IMU. For instance, the authors in [33] extend the ZUPT methodology to more general contexts for agents with other types of movements such as crawling, climbing, or jumping, while the authors in [34] use road-maps and topographic information to tune the agent's dynamic model. In summary, existing approaches incur additional complexities

Manuscript received January 19, 2015; revised August 20, 2015; accepted November 16, 2015. Date of publication January 06, 2016; date of current version April 27, 2016. The associate editor coordinating the review of this manuscript and approving it for publication was Prof. Marco Lops. This work is partially supported by the CDTI Spanish project TABON under Grant IDI-20140885, the Defense University Research Instrumentation Program under Grant N00014-08-1-0826, the Air Force Office of Scientific Research under Grant FA9550-12-0287, and the MIT Institute for Soldier Nanotechnologies.

J. Prieto is with the BISITE Research Group, University of Salamanca, 37008 Salamanca, Spain (e-mail: javierp@usal.es).

S. Mazuelas is with the Department of Research and Development, Qualcomm Technologies, Inc., San Diego, CA 92121 USA (e-mail: smazuela@qti.qualcomm.com).

M.Z. Win is with the Laboratory for Information and Decision Systems (LIDS), Massachusetts Institute of Technology, Cambridge, MA 02139 USA (e-mail: moewin@mit.edu).

Color versions of one or more of the figures in this paper are available online at <http://ieeexplore.ieee.org>.

Digital Object Identifier 10.1109/TSP.2016.2515065

(supplementary detection stages or auxiliary hardware), and exploit contextual information in an ad-hoc intuitive manner lacking a general and principled framework. Such a framework can result in navigation techniques that effectively utilize any contextual information.

In this paper, we present a general framework and algorithms for context-aided inertial navigation that exploit the available sources of information in a principled manner. Specifically, the main contributions of the paper are as follows.

- We establish a general framework for context-aided inertial navigation, and propose a principled methodology to incorporate general contextual information.
- We present a systematic approach to effectively exploit the contextual information by modeling such information as a potential function.
- We develop a recursive algorithm for context-aided inertial navigation based on the inference technique called belief condensation (BC) [35] that enables the implementation of the proposed framework.
- We demonstrate the performance improvements of the proposed methods in comparison to existing techniques via experimentation in the case study of indoor pedestrian navigation based on foot-mounted IMU.

The paper is organized as follows: Section II formulates the problem of inertial navigation and defines the system models; Section III describes the augmented graphical model that enables the incorporation of contextual information; Section IV presents algorithms to efficiently implement the proposed navigation framework via BC; Section V applies the general framework for the case study where the context is pedestrian walking with a foot-mounted IMU; Section VI assesses the performance of the presented techniques via experimentation in two indoor scenarios; finally, Section VII draws the conclusions.

*Notations:*  $\mathbf{x}_{1:k}$  denotes the sequence of random vectors  $\{\mathbf{x}_1, \mathbf{x}_2, \dots, \mathbf{x}_k\}$ ;  $[\cdot]^T$  denotes the transpose of its argument;  $\mathbf{I}_n$  denotes the  $n \times n$  identity matrix;  $\mathbb{H}$  denotes the set of quaternions; if  $\mathbf{p}, \mathbf{q} \in \mathbb{H}$ ,  $\mathbf{p} \odot \mathbf{q}$  and  $\exp(\mathbf{q})$  denote the quaternion multiplication and exponential, respectively, defined according to Appendix A;  $f(\mathbf{x})$  denotes the probability density function (pdf) or the probability mass function (pmf) of a continuous or discrete random variable  $\mathbf{x}$ , respectively; finally,  $\mathbf{x} \sim \mathcal{N}(\boldsymbol{\mu}, \boldsymbol{\Sigma})$  indicates that the random vector  $\mathbf{x}$  follows a Gaussian distribution with mean  $\boldsymbol{\mu}$  and covariance matrix  $\boldsymbol{\Sigma}$ , and  $\varphi(\mathbf{x}; \boldsymbol{\mu}, \boldsymbol{\Sigma})$  denotes the pdf of  $\mathbf{x}$ .

## II. INERTIAL NAVIGATION

In this section, we formulate the problem of inertial navigation in a three-dimensional scenario from IMU measurements. The corresponding graphical model is a hidden Markov model (HMM) that enables optimal recursive Bayesian filtering [36], [37].

### A. Problem Formulation

We assume a scenario where an agent carries an IMU that collects inertial measurements  $\{\mathbf{y}_k\}_{k \in \mathbb{N}}$ , at discrete time instants  $\{t_k\}_{k \in \mathbb{N}}$ . From these measurements, the goal is to estimate the agent's positional states  $\{\mathbf{x}_k\}_{k \in \mathbb{N}}$  that include its positions. The IMU provides measurements in its own

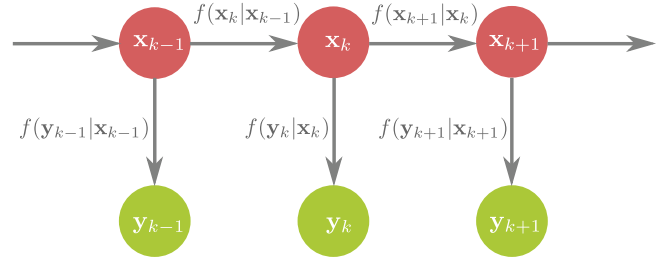


Fig. 1. HMM for states and measurements evolution. The relationship between  $\mathbf{x}_k$  and  $\mathbf{x}_{k-1}$ , and the relationship between  $\mathbf{y}_k$  and  $\mathbf{x}_k$  are the only two kinds of dependence.

body reference frame (moving) whereas the aim is to obtain the positional states in the navigation reference frame (fixed). Therefore, the positional state has to include the rotation from the navigation frame to the body frame, referred in this paper as orientation. The state also includes the first and second derivatives of position to relate the positional state and the measurements coming from the accelerometer. Similarly, it includes the first derivative of rotation to relate the positional state and the measurements coming from the gyroscope. In the following, we detail the specific components of both states and measurements.

The positional state of the agent at time  $t_k$  is  $\mathbf{x}_k = [\mathbf{p}_k, \mathbf{v}_k, \mathbf{a}_k, \mathbf{q}_k, \boldsymbol{\omega}_k, \mathbf{b}_k] \in \mathbb{R}^{22}$ , where  $\mathbf{p}_k \in \mathbb{R}^3$ ,  $\mathbf{v}_k \in \mathbb{R}^3$ ,  $\mathbf{a}_k \in \mathbb{R}^3$ ,  $\mathbf{q}_k \in \mathbb{H} \simeq \mathbb{R}^4$ , and  $\boldsymbol{\omega}_k \in \mathbb{R}^3$  denote position, velocity, acceleration, orientation, and angular velocity, respectively, all of them represented in the navigation reference frame.<sup>1</sup> The vector  $\mathbf{b}_k = [\mathbf{b}_k^f, \mathbf{b}_k^\omega] \in \mathbb{R}^6$  includes biases of the measurements collected by the accelerometers,  $\mathbf{b}_k^f \in \mathbb{R}^3$ , and the gyroscopes,  $\mathbf{b}_k^\omega \in \mathbb{R}^3$ .

The measurements vector is  $\mathbf{y}_k = [\mathbf{y}_k^f, \mathbf{y}_k^\omega] \in \mathbb{R}^6$ , where  $\mathbf{y}_k^f \in \mathbb{R}^3$  is the force measurement from the accelerometers, and  $\mathbf{y}_k^\omega \in \mathbb{R}^3$  is the angular velocity measurement from the gyroscopes.

### B. Hidden Markov Model

With the defined states and measurements, it can be assumed that given the current positional state,  $\mathbf{x}_k$ , the measurements vector,  $\mathbf{y}_k$ , is independent of all previous and future states and measurements [36]. Therefore, we can build an HMM determined by two kinds of dependence among the random variables: the relationship between the positional state at time  $t_k$  and the positional state at time  $t_{k-1}$ , i.e.,  $f(\mathbf{x}_k | \mathbf{x}_{k-1})$ , called *dynamic model*; and the relationship between the measurements and the positional state at each time, i.e.,  $f(\mathbf{y}_k | \mathbf{x}_k)$ , called *measurements model* (see Fig. 1) [36], [37].

This modeling as an HMM enables us to infer the positional state at time  $t_k$ ,  $\mathbf{x}_k$ , from the measurements up to time  $t_k$ ,  $\mathbf{y}_{1:k}$ , through a recursive process known as Bayesian filtering. In this process, the posterior distribution  $f(\mathbf{x}_k | \mathbf{y}_{1:k})$  is recursively determined from the previous posterior  $f(\mathbf{x}_{k-1} | \mathbf{y}_{1:k-1})$ , and

<sup>1</sup>The orientation  $\mathbf{q}_k$  represents a rotation from the navigation frame to the sensor body frame. Different orientation representations can be selected ranging from minimal three-dimensional vectors to nine-element rotation matrices [28], [38]. In this paper, we use the unit quaternion since it is the most concise and efficient representation for real-time navigation systems [39], [40].

the current measurements  $\mathbf{y}_k$ , by using the dynamic model,  $f(\mathbf{x}_k | \mathbf{x}_{k-1})$ , and the measurements model,  $f(\mathbf{y}_k | \mathbf{x}_k)$ , as follows [35]–[37]

$$f(\mathbf{x}_k | \mathbf{y}_{1:k}) \propto f(\mathbf{y}_k | \mathbf{x}_k) \int f(\mathbf{x}_k | \mathbf{x}_{k-1}) f(\mathbf{x}_{k-1} | \mathbf{y}_{1:k-1}) d\mathbf{x}_{k-1} \quad (1)$$

where  $f(\mathbf{x}_1 | \mathbf{x}_0) = f(\mathbf{x}_1)$ .

When the dynamic and measurements models are linear and Gaussian, recursion (1) can be implemented in closed-form via the celebrated Kalman filter (KF). When the system models are nonlinear or non-Gaussian, filtering techniques have to resort to approximations that deal with the complexity vs. accuracy trade-off, such as extended KFs (EKFs) [41], unscented KFs (UKFs) [42], particle filters (PFs) [37], and BC filters (BCFs) [35].

### C. Dynamic and Measurements Models

In the following, we describe the statistical models that characterize the HMM for inertial navigation.

1) *Dynamic Model*: The conditional pdf  $f(\mathbf{x}_k | \mathbf{x}_{k-1})$  models the dynamics of the positional state. Given the position, velocity, and acceleration at time  $t_{k-1}$ ,  $\mathbf{p}_{k-1}$ ,  $\mathbf{v}_{k-1}$ , and  $\mathbf{a}_{k-1}$ , the position, velocity, and acceleration at time  $t_k$ ,  $\mathbf{p}_k$ ,  $\mathbf{v}_k$ , and  $\mathbf{a}_k$ , can be modeled as

$$\begin{bmatrix} \mathbf{p}_k \\ \mathbf{v}_k \\ \mathbf{a}_k \end{bmatrix} = \begin{pmatrix} \mathbf{I}_3 & \Delta_k \mathbf{I}_3 & \frac{\Delta_k^2}{2} \mathbf{I}_3 \\ \mathbf{0} & \mathbf{I}_3 & \Delta_k \mathbf{I}_3 \\ \mathbf{0} & \mathbf{0} & \mathbf{I}_3 \end{pmatrix} \begin{bmatrix} \mathbf{p}_{k-1} \\ \mathbf{v}_{k-1} \\ \mathbf{a}_{k-1} \end{bmatrix} + \mathbf{n}_k^{\text{d},1} \quad (2)$$

where  $\Delta_k = (t_k - t_{k-1}) \in \mathbb{R}$  and  $\mathbf{n}_k^{\text{d},1} \in \mathbb{R}^9$  is the error term commonly modeled as white Gaussian noise [36].

Given the orientation and angular velocity at time  $t_{k-1}$ ,  $\mathbf{q}_{k-1}$  and  $\boldsymbol{\omega}_{k-1}$ , the orientation and angular velocity at time  $t_k$ ,  $\mathbf{q}_k$  and  $\boldsymbol{\omega}_k$ , can be modeled as<sup>2</sup>

$$\begin{bmatrix} \mathbf{q}_k \\ \boldsymbol{\omega}_k \end{bmatrix} = \begin{bmatrix} \exp\left(-\frac{\Delta_k}{2} \boldsymbol{\omega}_{k-1}^{\text{q}}\right) \odot \mathbf{q}_{k-1} \\ \boldsymbol{\omega}_{k-1} \end{bmatrix} + \begin{bmatrix} \mathbf{n}_k^{\text{d},2} \\ \mathbf{n}_k^{\text{d},3} \end{bmatrix} \quad (3)$$

where  $\boldsymbol{\omega}_{k-1}^{\text{q}} = [0, \boldsymbol{\omega}_{k-1}]$  [18], [30]. The terms  $\mathbf{n}_k^{\text{d},2}$  and  $\mathbf{n}_k^{\text{d},3}$  can be assumed to be four- and three-dimensional white Gaussian noise, respectively. Notice that this model is non-linear. In Section VI, we use its linearized version shown in Appendix B in accordance with the existing literature [30].

Given the biases at time  $t_{k-1}$ ,  $\mathbf{b}_{k-1}$ , the biases at time  $t_k$ ,  $\mathbf{b}_k$ , can be modeled as,

$$\mathbf{b}_k = \mathbf{b}_{k-1} + \mathbf{n}_k^{\text{d},4} \quad (4)$$

where the term  $\mathbf{n}_k^{\text{d},4} \in \mathbb{R}^6$  is modeled as white Gaussian noise.

In summary, the dynamic model  $f(\mathbf{x}_k | \mathbf{x}_{k-1})$  is Gaussian with mean given by the right-hand sides of (2), (3) and (4), and covariance given by the covariances  $\boldsymbol{\Sigma}_k^{\text{d},i}$  corresponding to  $\mathbf{n}_k^{\text{d},i}$ , for  $i = 1, 2, 3, 4$ , respectively.

<sup>2</sup>In (3) we assume that the direction of  $\boldsymbol{\omega}(t)$  is constant during the time interval between two measurements [39]. This is a mild assumption since MEMS-based IMUs provide measurements at frequencies around 100 Hz.

2) *Measurement Model*: The conditional pdf  $f(\mathbf{y}_k | \mathbf{x}_k)$  models the relationship between the state and measurements from accelerometers and gyroscopes.

The accelerometer integrated in the IMU provides force measurements in the sensor body frame,  $\mathbf{y}_k^{\text{f}} \in \mathbb{R}^3$  [28]. However, we want to estimate the acceleration in the navigation frame,  $\mathbf{a}_k$ . The relationship between both vectors is given by<sup>3</sup> [30]

$$\begin{aligned} \mathbf{y}_k^{\text{f}} &= \mathbf{f}_k + \mathbf{b}_k^{\text{f}} + \mathbf{n}_k^{\text{f}} \\ &= \mathbf{C}(\mathbf{q}_k)(\mathbf{a}_k - \mathbf{g}) + \mathbf{b}_k^{\text{f}} + \mathbf{n}_k^{\text{f}} \end{aligned} \quad (5)$$

where  $\mathbf{f}_k \in \mathbb{R}^3$  is the force in the sensor body frame,  $\mathbf{g} \in \mathbb{R}^3$  is the gravity, and  $\mathbf{C}(\mathbf{q}_k) \in \mathbb{R}^{3 \times 3}$  is the rotation matrix, which represents the same rotation as the unit quaternion  $\mathbf{q}_k$  and is given in Appendix A. The term  $\mathbf{n}_k^{\text{f}} \in \mathbb{R}^3$  is modeled as white Gaussian noise, and  $\mathbf{b}_k^{\text{f}} \in \mathbb{R}^3$  is the bias introduced by the sensor.

The gyroscope integrated in the IMU provides angular velocity measurements,  $\mathbf{y}_k^{\omega} \in \mathbb{R}^3$ , related to the positional state by,

$$\mathbf{y}_k^{\omega} = \boldsymbol{\omega}_k + \mathbf{b}_k^{\omega} + \mathbf{n}_k^{\omega} \quad (6)$$

where  $\mathbf{n}_k^{\omega} \in \mathbb{R}^3$  is modeled as white Gaussian noise and  $\mathbf{b}_k^{\omega} \in \mathbb{R}^3$  is the bias introduced by the sensor.

In summary, the measurements model  $f(\mathbf{y}_k | \mathbf{x}_k)$  is Gaussian with mean given by the right-hand sides of (5) and (6), and covariance given by the covariances  $\boldsymbol{\Sigma}_k^{\text{f}}$  and  $\boldsymbol{\Sigma}_k^{\omega}$  corresponding to  $\mathbf{n}_k^{\text{f}}$  and  $\mathbf{n}_k^{\omega}$ , respectively.

## III. CONTEXTUAL KNOWLEDGE

In this section, we augment the HMM described in the previous section to incorporate contextual knowledge.

### A. Graphical Model for Context-Aided Inertial Navigation

Let  $c_k$  be the context of the agent at time  $t_k$ . Such a context can take different values depending on the circumstances at time  $t_k$ . For instance,  $c_k$  can specify the part of the body where the agent carries the IMU (e.g., foot, waist, and chest), the motion patterns (e.g., walking, running, and jumping), or the navigation environment (e.g., corridor, ramp, and elevator).<sup>4</sup> The context can be provided by external inputs such as the agent itself, or estimated by identifiers such as image classification methods [43].

With the defined states, measurements, and contexts, it can be assumed that given the current positional state,  $\mathbf{x}_k$ , the measurements vector and context,  $\mathbf{y}_k$  and  $c_k$ , are independent. Notice that the state vector includes acceleration, orientation, angular velocity, and biases; therefore, the previous conditional independence assumption only implies that the white Gaussian noises in (5) and (6) are independent of the context. In addition, analogously to the previous section, given the current positional

<sup>3</sup>We consider that the region of interest is small enough to assume a negligible Earth's rotation and constant gravity [40].

<sup>4</sup>For example, the context,  $c_k$ , can take the value “the agent is a human walking inside the Louvre with the IMU on his or her foot.”

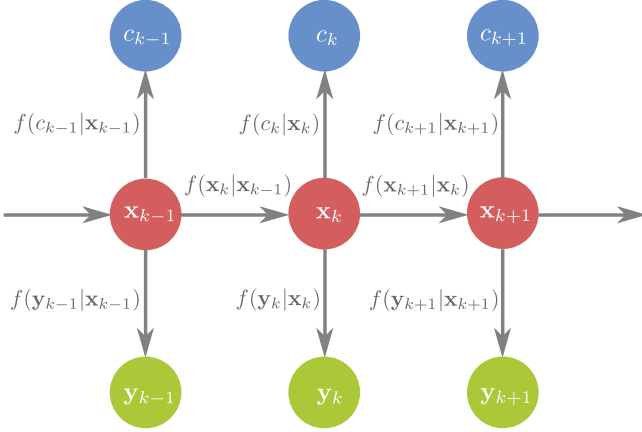


Fig. 2. Graphical model for measurements, states and context evolution. The HMM shown in Fig. 1 is augmented to include contextual information.

state, current measurements and contexts can be assumed to be independent of all previous and future states, measurements, and contexts. These conditional independences allow us to represent the evolution in time of states, measurements, and contexts by the graphical model shown in Fig. 2. This augmented graphical model enables us to include contextual information while keeping a tree-structure that allows for optimal recursive computation of posterior distributions [44].

The relationship between the context and the state at time  $t_k$  can be described by the potential function  $f(c_k | \mathbf{x}_k)$ . For each specific context, such a potential is a function of the state,<sup>5</sup> i.e.,  $f(c_k | \mathbf{x}_k) = f(c_k | \mathbf{P}_k \mathbf{x}_k)$ , where  $\mathbf{P}_k$  is a matrix projecting the components of  $\mathbf{x}_k$  into the relevant components for the context  $c_k$ . In the remaining of this section, we drop the subindex  $k$  for notational convenience.

### B. Context Modeling

For each context  $c_k$ , the potential  $f(c_k | \mathbf{x}_k)$  is a function of  $\mathbf{x}_k$ . Notice that the context does not necessarily influence all the variables in the state,<sup>5</sup> i.e.,  $f(c_k | \mathbf{x}_k) = f(c_k | \mathbf{P}_k \mathbf{x}_k)$ , where  $\mathbf{P}_k$  is a matrix projecting the components of  $\mathbf{x}_k$  into the relevant components for the context  $c_k$ . In the remaining of this section, we drop the subindex  $k$  for notational convenience.

By using Bayes' rule, we have

$$f(c | \mathbf{x}) = f(c | \mathbf{P}\mathbf{x}) \propto \frac{f(\mathbf{P}\mathbf{x} | c)}{f(\mathbf{P}\mathbf{x})}. \quad (7)$$

Therefore, for each context, an estimate of the potential function  $f(c | \mathbf{x})$  can be found from an estimate of the density corresponding to the context-relevant state components  $f(\mathbf{P}\mathbf{x} | c)$ . When no relevant prior knowledge about the positional state components  $\mathbf{P}\mathbf{x}$  is available, the distribution  $f(\mathbf{P}\mathbf{x})$  can be assumed constant and an estimate of the potential function,

<sup>5</sup>For instance, only velocities, accelerations, and angular velocities are influenced by the context of a pedestrian walking with a foot-mounted IMU.

$f(c | \mathbf{x})$ , can be directly obtained from an estimate of the density  $f(\mathbf{P}\mathbf{x} | c)$ .<sup>6</sup> When relevant prior knowledge about the positional state components  $\mathbf{P}\mathbf{x}$  is available, the prior  $f(\mathbf{P}\mathbf{x})$  accounts for this knowledge in (7), and an estimate of  $f(c | \mathbf{x})$  can be obtained from the estimate of the density  $f(\mathbf{P}\mathbf{x} | c)$  divided by such prior knowledge.

Let  $\mathbf{P}\mathbf{x} \in \mathbb{R}^D$  with  $D \leq \dim(\mathbf{x})$ , a general density estimate of  $f(\mathbf{P}\mathbf{x} | c)$  can be represented as a mixture, i.e.,

$$\hat{f}(\mathbf{P}\mathbf{x} | c) = \sum_{i=1}^{m(c)} \alpha_i(c) g_i(\mathbf{P}\mathbf{x}; \boldsymbol{\theta}(c)) \quad (8)$$

where  $\alpha_1(c), \alpha_2(c), \dots, \alpha_{m(c)}(c) \in \mathbb{R}^+$ ,  $\sum_{i=1}^m \alpha_i(c) = 1$ , and  $g_i(\mathbf{P}\mathbf{x}; \boldsymbol{\theta}(c))$  is a pdf parametrized by some  $\boldsymbol{\theta}(c)$ . The mixture form in (8) covers density estimates based on kernels and mixtures of Gaussians [45]–[48]. The modeling as a mixture also helps interpretation both in terms of components and mixture weights. For example, in the case where the context corresponds to a foot-mounted IMU, a simple model for the density  $\hat{f}(\mathbf{P}\mathbf{x} | c)$  can be obtained as the sum of two components corresponding to the stance and swing phases of the foot in pedestrian movement. In addition, one component can model lateral walking where a small weight indicates little likelihood of such a type of walking.

As we describe in the following, the density estimate  $\hat{f}(\mathbf{P}\mathbf{x} | c)$  can be obtained by an expert-based or by a learning-based modeling of the context. In the former case, the mixture components can be approximated based on the logical constraints imposed by the context. In the latter case, the mixture parameters can be estimated by density estimation techniques [48] such as the Expectation-Maximization (EM) algorithm [49]. In both cases, considering a Gaussian kernel for the mixture components and unavailable prior knowledge about the states, the estimated potential function is given by

$$\hat{f}(c | \mathbf{x}) \propto \sum_{i=1}^{m(c)} \alpha_i(c) \varphi(\mathbf{P}\mathbf{x}; \boldsymbol{\mu}_i(c), \boldsymbol{\Sigma}_i(c)) \quad (9)$$

where  $\boldsymbol{\mu}_i(c) \in \mathbb{R}^D$  and  $\boldsymbol{\Sigma}_i(c) \in \mathbb{R}^{D \times D}$  are, respectively, the mean vector and covariance matrix of the  $i$ th component in the mixture.

In the following section, we present a recursive algorithm for context-aided inertial navigation based on BC and the augmented HMM. In Section V, we obtain estimates of the potential function  $f(c | \mathbf{x})$  using both expert-based and learning-based modeling for the context corresponding to a pedestrian walking with a foot-mounted IMU.

## IV. CONTEXT-AIDED INERTIAL NAVIGATION

The graphical model depicted in Fig. 2 allows for recursive computation of posterior distributions, analogously to the HMM of Section II. In this section, we describe a generalized framework for Bayesian inference under such a graphical model and provide an efficient implementation based on BC.

<sup>6</sup>Note that for Bayesian inference such a potential function just needs to be known up to a proportionality constant.

### A. Bayesian Inference for Context-Aided Inertial Navigation

The inference process described in Section II.B can be generalized to incorporate contextual information as follows. The graphical model for positional states, measurements, and contexts depicted in Fig. 2 accounts for the following factorization of the corresponding probability distributions,

$$\begin{aligned} f(\mathbf{x}_{1:k}, \mathbf{y}_{1:k}, c_{1:k}) &= f(\mathbf{x}_1) f(\mathbf{y}_1, c_1 | \mathbf{x}_1) \prod_{i=2}^k f(\mathbf{x}_i | \mathbf{x}_{i-1}) f(\mathbf{y}_i, c_i | \mathbf{x}_i) \\ &= f(\mathbf{x}_{1:k-1}, \mathbf{y}_{1:k-1}, c_{1:k-1}) f(\mathbf{x}_k | \mathbf{x}_{k-1}) f(\mathbf{y}_k, c_k | \mathbf{x}_k). \end{aligned} \quad (10)$$

In addition, as described in Section III.A, contexts and measurements can be assumed to be independent conditioned on the current positional state. That is,

$$\begin{aligned} f(\mathbf{y}_k, c_k | \mathbf{x}_k) &= f(\mathbf{y}_k | \mathbf{x}_k) f(c_k | \mathbf{y}_k, \mathbf{x}_k) \\ &= f(\mathbf{y}_k | \mathbf{x}_k) f(c_k | \mathbf{x}_k). \end{aligned}$$

Therefore, the posterior distribution of the positional state at time  $t_k$  given measurements and contexts up to time  $t_k$ ,  $f(\mathbf{x}_k | \mathbf{y}_{1:k}, c_{1:k})$ , can be obtained as

$$f(\mathbf{x}_k | \mathbf{y}_{1:k}, c_{1:k}) \propto f(\mathbf{y}_k | \mathbf{x}_k) f(c_k | \mathbf{x}_k) \cdot \int f(\mathbf{x}_k | \mathbf{x}_{k-1}) f(\mathbf{x}_{k-1} | \mathbf{y}_{1:k-1}, c_{1:k-1}) d\mathbf{x}_{k-1}. \quad (11)$$

Algorithm 1 shows the pseudocode of the proposed Bayesian inference for context-aided inertial navigation. In Algorithm 1, we recursively obtain the  $k$ th posterior distribution,  $f(\mathbf{x}_k | \mathbf{y}_{1:k}, c_{1:k})$ , from the  $(k-1)$ th posterior together with new measurements and context at time  $t_k$ .

---

#### Algorithm 1: Bayesian Inference for Context-aided Inertial Navigation.

---

- 1: INITIALIZATION:
- 2: Set  $\pi$  equal to the prior distribution of  $\mathbf{x}_1$ .
- 3: RECURSIVE BAYESIAN INFERENCE:
- 4: **for**  $k = 1, 2, \dots$  **do**
- 5: (i) FORWARD RECURSION:

$$\pi \leftarrow f(\mathbf{y}_k | \mathbf{x}_k) f(c_k | \mathbf{x}_k) \int f(\mathbf{x}_k | \mathbf{x}_{k-1}) \pi d\mathbf{x}_{k-1}$$

- 6: (ii) NORMALIZATION:

$$\pi \leftarrow \frac{\pi}{\int \pi d\mathbf{x}_k}$$

- 7: **return**  $\mathbb{E}\{\mathbf{x}_k | \mathbf{y}_{1:k}, c_{1:k}\} \leftarrow \mathbb{E}\pi\{\mathbf{x}_k\}$
  - 8: **end for**
- 

### B. Efficient Implementation of Context-Aided Inertial Navigation

The Bayesian inference for context-aided inertial navigation described in Algorithm 1 is not directly implementable due to

the lack of closed-form expressions for (11). In addition, the specific nature of contextual data together with low complexity requirements for real-time implementation prevent the usage of conventional approximation techniques. On the one hand, Kalman-like approaches such as EKF [41] and UKF [42] would require an explicit model relating contexts and states of the form  $c_k = h(\mathbf{x}_k) + n$ . Such an explicit model is hardly accessible due to the qualitative nature of contexts, and it is not needed to obtain the potential  $f(c_k | \mathbf{x}_k)$ . On the other hand, Monte Carlo-based approaches such as PF [37] would require complexities unaffordable for real-time operation due to the high dimensionality of the state [35], [50]. In particular, the state for context-aided inertial navigation is 22-dimensional and the complexity of PF increases exponentially with the state dimension; notice that PFs already require a number of particles in the order of  $10^5$  for problems with less than 10 dimensions [35], [50].

BC techniques have been recently proposed [35] showing a remarkable performance in terms of the complexity vs. accuracy trade-off. In particular, these techniques do not suffer from the limitations described above and can be readily used with the models shown in Sections II and III while keeping moderate complexities.

In the following, we first briefly describe the concept of BC in the setting of context-aided inertial navigation and then present the efficient implementation of Algorithm 1 based on BC.

### C. Context-Aided Inertial Navigation via Belief Condensation

The recursion given by (11) can be viewed as a mapping  $\Phi$  between probability distributions. Due to the lack of closed-form solutions for (11), each implementable inference technique, in turn, can be viewed as a mapping  $\hat{\Phi}$  that approximates the exact mapping  $\Phi$  under tractability constraints. The implementation constraints require that inputs and outputs of such a mapping  $\hat{\Phi}$  belong to tractable families of distributions. Arguments analogous to those given in [35] show that inference techniques that optimally deal with the complexity vs. accuracy trade-off are characterized as

$$\hat{\Phi}(g) \in \arg \min_{\tilde{f} \in \mathcal{F}} \{D(\Phi(g), \tilde{f})\} \quad (12)$$

where  $\mathcal{F}$  and  $D$  are a chosen tractable family of distributions and a discrepancy function, respectively.

Under the complexity constraints imposed by a real-time navigation system, the tractability of Gaussian family favors its selection as the family of distributions for the implementation of BC. The following result together with Algorithm 2 show how BC can be implemented for context-aided inertial navigation by approximating the posterior distribution  $f(\mathbf{x}_k | \mathbf{y}_{1:k}, c_{1:k})$  as a Gaussian distribution for each time step  $k$ .

*Proposition 1:* Let  $\pi$  be an approximation of  $f(\mathbf{x}_{k-1} | \mathbf{y}_{1:k-1}, c_{1:k-1})$ , and

$$\Phi(\pi) \propto f(\mathbf{y}_k | \mathbf{x}_k) f(c_k | \mathbf{x}_k) \int f(\mathbf{x}_k | \mathbf{x}_{k-1}) \pi d\mathbf{x}_{k-1}.$$

If  $\mathcal{F}$  is the family of Gaussian distributions and  $D_{\text{KL}}$  is the Kullback-Leibler (KL) divergence, then

$$\varphi(\mathbf{x}_k; \boldsymbol{\mu}_\pi, \boldsymbol{\Sigma}_\pi) = \arg \min_{\tilde{f} \in \mathcal{F}} \{D_{\text{KL}}(\Phi(\pi), \tilde{f})\} \quad (13)$$

**Algorithm 2:** BC for Context-aided Inertial Navigation.

- 1: INITIALIZATION:
- 2: Set  $\pi$  equal to the prior distribution of  $\mathbf{x}_1$ .

$$\begin{aligned}\boldsymbol{\mu}_\pi &\leftarrow \mathbb{E}\{\mathbf{x}_1\} \\ \boldsymbol{\Sigma}_\pi &\leftarrow \mathbb{E}\{\mathbf{x}_1\mathbf{x}_1^\top\} - \boldsymbol{\mu}_\pi\boldsymbol{\mu}_\pi^\top\end{aligned}$$

- 3:  $\pi \leftarrow \varphi(\mathbf{x}_1; \boldsymbol{\mu}_\pi, \boldsymbol{\Sigma}_\pi)$
- 4: RECURSIVE BAYESIAN INFERENCE:
- 5: **for**  $k = 1, 2, \dots$  **do**
- 6: Belief Condensation of  $\Phi(\pi)$

$$\pi^+ \leftarrow \int f(\mathbf{x}_k | \mathbf{x}_{k-1})\pi \, d\mathbf{x}_{k-1}$$

$$C \leftarrow \int f(\mathbf{y}_k | \mathbf{x}_k)f(c_k | \mathbf{x}_k)\pi^+ \, d\mathbf{x}_k$$

$$\begin{aligned}\boldsymbol{\mu}_\pi &\leftarrow \mathbb{E}_{\Phi(\pi)}\{\mathbf{x}_k\} \\ &= \frac{1}{C} \int \mathbf{x}_k f(\mathbf{y}_k | \mathbf{x}_k)f(c_k | \mathbf{x}_k)\pi^+ \, d\mathbf{x}_k\end{aligned}$$

$$\begin{aligned}\boldsymbol{\Sigma}_\pi &\leftarrow \mathbb{E}_{\Phi(\pi)}\{\mathbf{x}_k\mathbf{x}_k^\top\} - \boldsymbol{\mu}_\pi\boldsymbol{\mu}_\pi^\top \\ &= \frac{1}{C} \int \mathbf{x}_k\mathbf{x}_k^\top f(\mathbf{y}_k | \mathbf{x}_k)f(c_k | \mathbf{x}_k)\pi^+ \, d\mathbf{x}_k - \boldsymbol{\mu}_\pi\boldsymbol{\mu}_\pi^\top\end{aligned}$$

- 7:  $\pi \leftarrow \varphi(\mathbf{x}_k; \boldsymbol{\mu}_\pi, \boldsymbol{\Sigma}_\pi)$
- 8: **return**  $\mathbb{E}\{\mathbf{x}_k | \mathbf{y}_{1:k}, c_{1:k}\} \leftarrow \mathbb{E}_\pi\{\mathbf{x}_k\} = \boldsymbol{\mu}_\pi$
- 9: **end for**

where

$$\begin{aligned}\boldsymbol{\mu}_\pi &= \mathbb{E}_{\Phi(\pi)}\{\mathbf{x}_k\} \\ &= \frac{\int \mathbf{x}_k f(\mathbf{y}_k | \mathbf{x}_k)f(c_k | \mathbf{x}_k) \left( \int f(\mathbf{x}_k | \mathbf{x}_{k-1})\pi \, d\mathbf{x}_{k-1} \right) \, d\mathbf{x}_k}{\int f(\mathbf{y}_k | \mathbf{x}_k)f(c_k | \mathbf{x}_k) \left( \int f(\mathbf{x}_k | \mathbf{x}_{k-1})\pi \, d\mathbf{x}_{k-1} \right) \, d\mathbf{x}_k}\end{aligned}\quad (14)$$

and

$$\begin{aligned}\boldsymbol{\Sigma}_\pi &= \mathbb{E}_{\Phi(\pi)}\{\mathbf{x}_k\mathbf{x}_k^\top\} - \boldsymbol{\mu}_\pi\boldsymbol{\mu}_\pi^\top \\ &= \frac{\int \mathbf{x}_k\mathbf{x}_k^\top f(\mathbf{y}_k | \mathbf{x}_k)f(c_k | \mathbf{x}_k) \left( \int f(\mathbf{x}_k | \mathbf{x}_{k-1})\pi \, d\mathbf{x}_{k-1} \right) \, d\mathbf{x}_k}{\int f(\mathbf{y}_k | \mathbf{x}_k)f(c_k | \mathbf{x}_k) \left( \int f(\mathbf{x}_k | \mathbf{x}_{k-1})\pi \, d\mathbf{x}_{k-1} \right) \, d\mathbf{x}_k} \\ &\quad - \boldsymbol{\mu}_\pi\boldsymbol{\mu}_\pi^\top.\end{aligned}\quad (15)$$

*Proof:* The result is a consequence of the Corollary 1 in [35] for  $m = 1$ .  $\square$

The implementation of BC for context-aided inertial navigation amounts to compute in each time step the four 22-dimensional integrals in stage 6 of Algorithm 2, i.e., (14) and (15). These integrals can be numerically approximated through Monte Carlo integration or by efficient quadrature rules that exploit the fact that they are integrals with respect to Gaussians [51]. Notice, for example, that  $\int f(\mathbf{x}_k | \mathbf{x}_{k-1})\pi \, d\mathbf{x}_{k-1}$  in stage 6 of Algorithm 2 has a simple closed-form expression using the linearized version of the dynamic model  $f(\mathbf{x}_k | \mathbf{x}_{k-1})$  since  $\pi$  is Gaussian.

The above BC-based implementation enables inertial navigation under the graphical model augmented with contextual information. Next section particularizes the general framework presented and specifies the context modeling for the case study of a pedestrian walking with a foot-mounted IMU.

## V. CASE STUDY: PEDESTRIAN NAVIGATION WITH A FOOT-MOUNTED IMU

In this section, we evaluate the proposed techniques through the case study of pedestrian navigation based on foot-mounted IMU inertial measurements. In this case study, the context represents the fact that the IMU is mounted on the pedestrian's foot and is constant for all time steps. This context is the most studied in the literature and hence enables a proper assessment of the methods presented in this paper. In comparison to existing approaches [19]–[26], we show that the proposed techniques can capture the contextual information and fully exploit the available measurements leading to a more accurate pedestrian navigation.

### A. Existing Approaches

The movement of the foot whilst walking is comprised of two distinguished phases: stance phase (i.e., staying on the ground), and swing phase (i.e., moving in the air), where the stance phase is characterized by very low values of velocity, acceleration, and angular velocity. Conventional approaches use this knowledge to mitigate the drift in navigation [19]–[26].

Existing techniques mitigate velocity drifts by detecting stance phases from measurements collected by both accelerometers and gyroscopes [19]–[24]. For example, the procedure shown in [22] imposes certain thresholds on the magnitude and variance of the force and on the magnitude of the angular velocity. Other schemes that incorporate additional hardware detect stance phases from measurements provided by shoe-embedded radar or RF sensors [16], [25], [26]. For example, the procedure shown in [26] sets different thresholds on the position and velocity relative to the ground.

When the foot is assumed to be in a stance phase, conventional approaches utilize this knowledge to correct the estimated velocity (the so-called ZUPT). This correction is accomplished before position integration by resetting the current estimated velocity to zero, taking into account that the foot is motionless during the stance phase [19]–[24].

As described in previous sections, the proposed framework enables a more principled treatment of the contextual information by incorporating such information in the Bayesian inference process through the potential function  $f(c_k | \mathbf{x}_k)$  that can be approximated as

$$\hat{f}(c_k | \mathbf{x}_k) = \sum_{i=1}^m \alpha_i \varphi(\mathbf{P}_k \mathbf{x}_k; \boldsymbol{\mu}_i, \boldsymbol{\Sigma}_i) \quad (16)$$

where the right-hand side does not show the dependence with  $c_k$  because in this section we only consider one context. In the following, we describe such a potential function that models the specific context of pedestrian navigation with a foot-mounted IMU.

### B. Expert-Based Context Modeling

Using a similar expert knowledge as the one used by ZUPT-based approaches, the potential function at a time instant  $t_k$ ,  $f(c_k | \mathbf{x}_k)$ , can be approximated by a mixture with two components corresponding to stance and swing phases. By selecting a Gaussian kernel, the potential function for the positional state at time  $t_k$  for the specific context herein considered is

$$\begin{aligned}\hat{f}(c_k | \mathbf{x}_k) &= \hat{f}(c_k | \mathbf{P}_k \mathbf{x}_k) \\ &\propto \alpha \varphi(\mathbf{P}_k \mathbf{x}_k; \mathbf{0}, \boldsymbol{\Sigma}_1) + (1 - \alpha) \varphi(\mathbf{P}_k \mathbf{x}_k; \mathbf{0}, \boldsymbol{\Sigma}_2)\end{aligned}\quad (17)$$

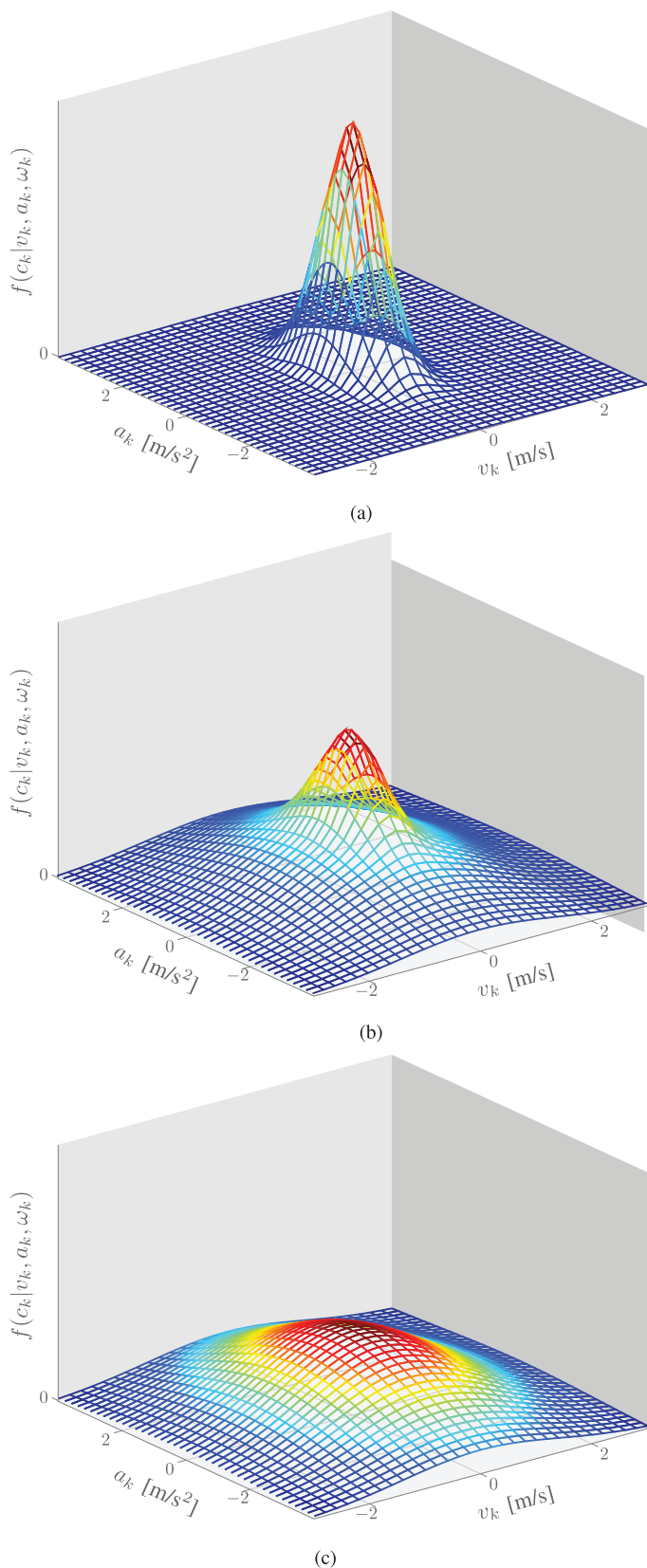


Fig. 3. The phases of the foot whilst walking allow the recognition of velocity, acceleration and angular velocity potential function characterizing stance and swing phases. Such a function can be modeled by expert knowledge, assigning a narrow component to the first and a wide component to the second. (a)  $\omega_k \approx 0$  rad/s, (b)  $\omega_k \gtrsim 0$  rad/s, (c)  $\omega_k \gg 0$  rad/s.

where  $\mathbf{P}_k \mathbf{x}_k = [v_k, \mathbf{a}_k, \omega_k]$ ,  $\Sigma_1$  and  $\Sigma_2$  are the covariance matrices for the Gaussian pdfs modeling the stance and swing phases, respectively, and  $\alpha \in [0, 1]$  is the probability of occurrence of the first. The covariances satisfy  $\Sigma_1 \prec \Sigma_2$  so that the component related to the stance phase imposes much higher odds to low values of the variables.

In order to describe how this expert-based potential function establishes soft constraints onto the positional state, we plot in Fig. 3 its behavior in a one-dimensional case. This figure represents the variation of the potential function given three specific values of angular velocity for  $\alpha = 0.5$ . We selected two diagonal covariances with standard deviation regarding velocity, acceleration and angular velocity of 0.05 m/s, 0.3 m/s<sup>2</sup> and 0.2 rad/s, respectively, for the stance phase and 2.5 m/s, 7.5 m/s<sup>2</sup> and 2 rad/s, respectively, for the swing phase. When the acceleration and the angular velocities take values close to zero, the potential of low velocities is significantly larger than the potential of high velocities, i.e., the narrower component in the mixture is dominant over the wider component in the mixture. When the acceleration or the angular velocity become higher, the potential of low velocities is similar to the potential of high velocities, i.e., the wider component in the mixture is dominant over the narrower component in the mixture.

In the following, we describe a systematic methodology for learning-based context modeling that can exploit more complex relationships among the state variables and does not rely on expert knowledge about the context.

### C. Learning-Based Context Modeling

The movement pattern of a bipedal walk is more complex than a simple combination of stance and swing phases [52]. This is manifested in Fig. 4(a) that shows the module of velocity, acceleration and angular velocity values estimated for a 5-minutes' walk with a foot-mounted IMU.<sup>7</sup> Fig. 4(a) shows that bipedal walk imposes clear constraints on velocities, accelerations, and angular velocities, leading to a complex behavior of the values of these variables. In the following, we detail the training phase to learn the model describing the constraints imposed by the context, that is, the potential function  $f(c_k | \mathbf{x}_k)$ .

Let  $\{\mathbf{x}^{(n)}\}_{n=1}^N$  be a set of positional states obtained in a specific context  $c$ , the distribution  $f(\mathbf{P}\mathbf{x} | c)$  (and hence the potential function  $f(c | \mathbf{x}) = f(c | \mathbf{P}\mathbf{x})$ ) can be learned from those positional states through density estimation. In this paper, we model the distribution  $f(\mathbf{P}\mathbf{x} | c)$  as a mixture of Gaussians and obtain its parameters by using the EM algorithm [53]. Fig. 4 compares the conventional 2-component (stance and swing) clustering of state values and a more intricate 4-components mixture approach. Fig. 4(a) shows the module of estimated values of velocity, acceleration and angular velocity. Fig. 4(b) illustrates the stance and swing clusters resulting from the thresholds imposed by conventional approaches. Fig. 4(c) depicts the proposed 4-component clustering based on the EM algorithm. The last figure reflects that the proposed

<sup>7</sup>The estimation of such variables was carried out by using a conventional inertial navigation technique based on EKF and ZUPT [21]–[24].

approach is not only able to correctly model stance phase by a single mixture component, but also obtains other 3 mixture components that aids the navigation performance as we show in the next section.<sup>8</sup>

## VI. PERFORMANCE EVALUATION

In this section, we assess the performance of the navigation framework presented in this paper using the case study described in Section V. In the following, we characterize the setup for the experiments and present the performance results in comparison with existing techniques.

### A. Experimental Setup

The performance evaluation is based on measurements obtained using the commercial XSens MTi IMU (based on MEMS technology) working at the frequency of 100 Hz ( $\Delta_k = 0.01$  s). We obtained experimental data in two indoor scenarios from different pedestrians subject to the selected foot-mounted IMU context. Fig. 5 shows the map plans of the two scenarios together with the respective trajectories followed by the agents.

In the first scenario (see Fig. 5(a)), the agent walked slowly with gentle movements completing a route of 320 meters in approximately 7 minutes with an average speed of 0.8 m/s and smooth turns. Along this route, the agent stopped and sat down for approximately 25 seconds at the place marked as “SEAT”.

In the second scenario (see Fig. 5(b)), the agent walked fast with sudden movements completing a route of 435 meters in approximately 7 minutes with an average speed of 1.1 m/s and abrupt turns. Along this route, the agent stopped and stood still between 5 and 10 seconds in the 5 places marked as “STOP”.

Table I summarizes the values assigned to the covariances of the dynamic and measurements models defined in Section II.C. Dynamic-related values are roughly 50% of their maximum, which is a common practice in tracking applications [36]. Measurement-related values come from specification, which is commonly found in manufacturer’s certificate.

We used the learning-based context modeling described in Section V.C. Specifically, the initialization of the EM algorithm was obtained as the expert-based mixture shown in Section V.B, and the samples used by the EM algorithm were the state estimates obtained by a conventional implementation based on EKF and ZUPT. In addition, we tested the performance of the proposed techniques by using 2-fold cross validation where we used the first scenario for training and the second scenario for testing, and vice-versa.

### B. Results and Discussion

We use the center of the corridors as a proxy for the actual trajectory due to the inherent difficulty of knowing the exact ground-truth. Then, for each trajectory, we use two

<sup>8</sup>In Fig. 4(c), the cluster corresponding to the stance phase contains 36% of observed states. This component has a mean vector close to zero and a covariance matrix with standard deviation values of 0.03 m/s, 0.3 m/s<sup>2</sup> and 0.15 rad/s for velocity, acceleration and angular velocity components, respectively.

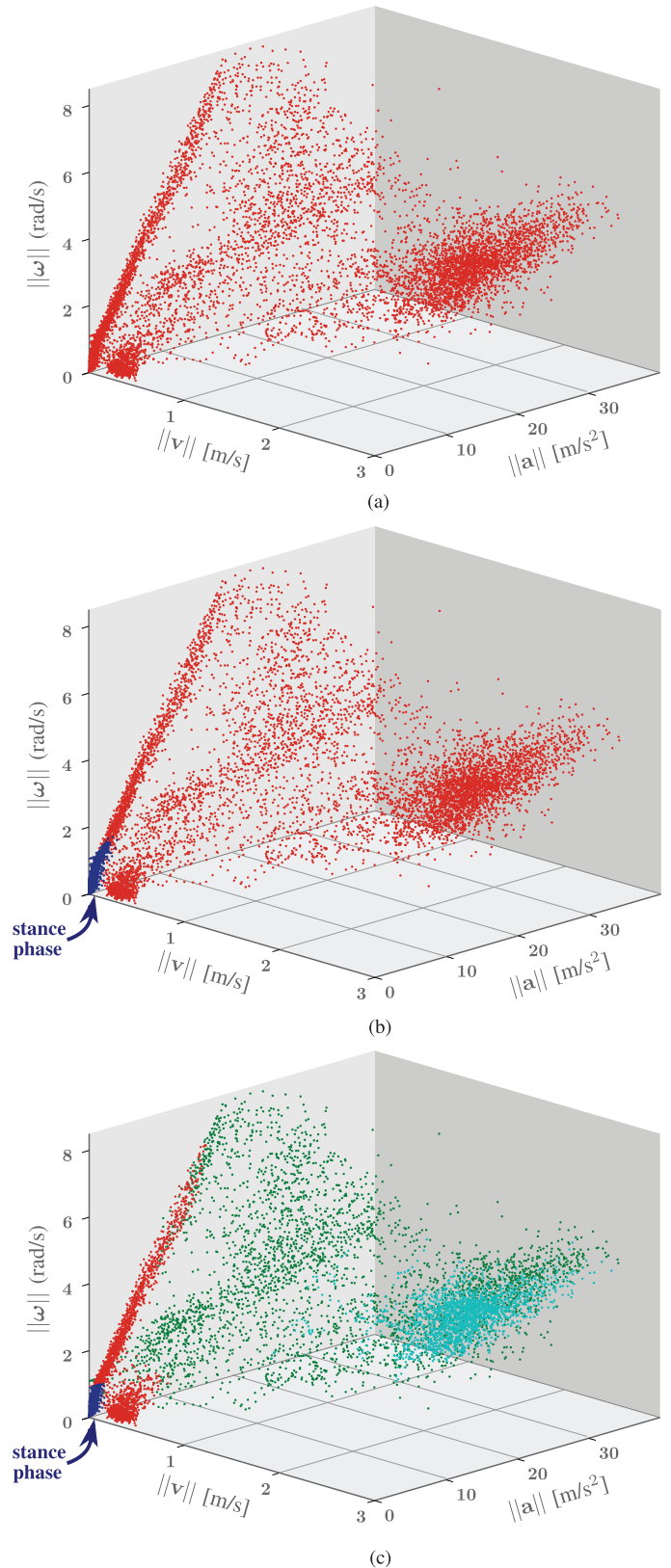


Fig. 4. The phases of the foot whilst walking allow the division of velocity, acceleration and angular velocity values into clusters or components. A mixture of such components can be obtained from previously observed states, enabling the approximation of the potential function representing the context influence. (a) Original data, (b) Conventional threshold-based clustering, (c) Proposed EM-based clustering.



Fig. 5. The proposed context modeling avoids the rapid growth of the error over time of conventional approaches, resulting in a very high (sub-meter) accuracy. (a) Smooth movements, (b) Abrupt movements.

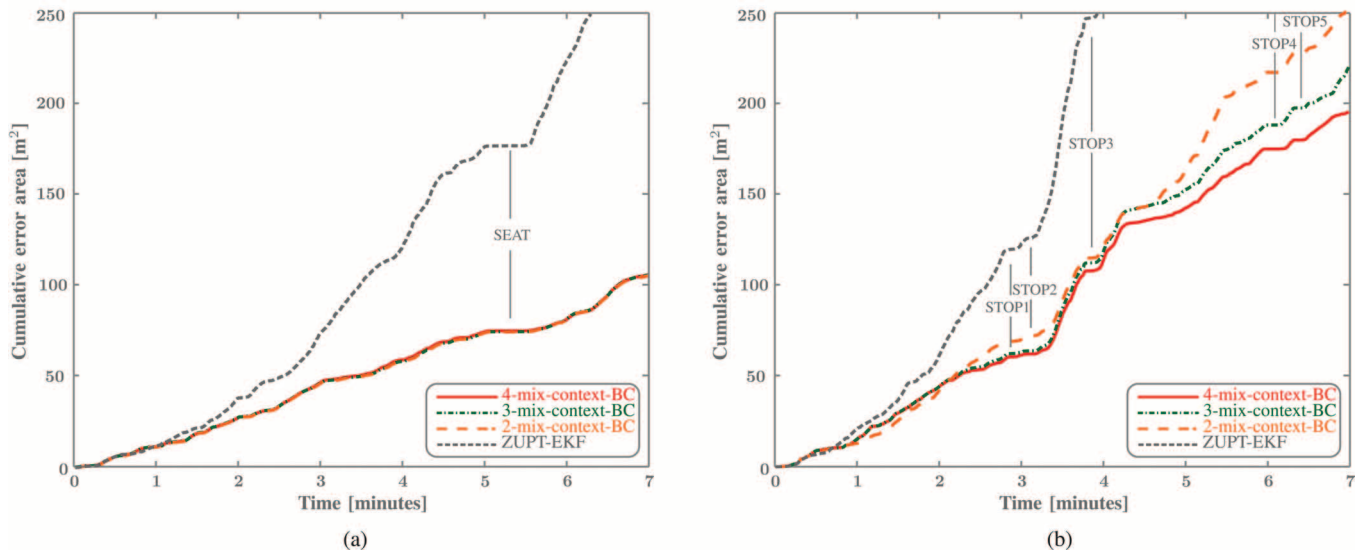


Fig. 6. The drift between the actual path and the position estimates is significantly smaller using the proposed techniques compared to conventional approaches. In addition, increasing the complexity of context modeling (number of components in the mixture) results in enhanced performance in cases with abrupt movements. (a) Smooth movements, (b) Abrupt movements.

performance metrics obtained from the estimated trajectory and the trajectory formed by the center of the corridors: 1) the time-varying accumulated area between both trajectories (“cumulative error area”), and 2) the instantaneous distance between both trajectories (“error bar”). In the following we denote

- *m*-mix-context-BC (proposed): the positions are estimated with the presented BC-based algorithm by fusing inertial measurements and a *m*-component mixture modeling of the context.
- ZUPT-EKF (conventional): the positions are estimated with an implementation of conventional pedestrian navigation techniques based on ZUPT [18]–[26]. Specifically, stance phases are detected from online inertial measurements as in [18]–[24]; filtering is implemented using an EKF as in [21]–[24]; the detection of stance phases is carried out by thresholds imposed to a measurements window

as in [22]; and the zero velocity updates are performed as in [18].

In order to ensure a fair comparison, both proposed and conventional techniques use the dynamic and measurements models shown in Section II.C.

The complexity of both techniques is similar since both use Gaussian distributions to characterize posteriors. Specifically, the BC-based method requires performing additional numerical integration as described in Section IV.C while the ZUPT-based method requires performing additional stance/swing phases detection over a window of inertial measurements. For both techniques, the processing time is on the order of tens of milliseconds, which allows for real-time implementation at the data acquisition rate of 100 Hz.

Figs. 5 and 6 as well as Table II summarize the results of the proposed and conventional approaches over the two mentioned scenarios.

TABLE I  
 EXPERIMENTAL VALUES FOR PERFORMANCE EVALUATION

Covariance	Experimental value
$\Sigma_k^{d,1}$	$275 \cdot \begin{pmatrix} \frac{\Delta_k^3}{6} \mathbf{I}_3 \text{ m/s} & \mathbf{0} & \mathbf{0} \\ \mathbf{0} & \frac{\Delta_k^2}{2} \mathbf{I}_3 \text{ m/s}^2 & \mathbf{0} \\ \mathbf{0} & \mathbf{0} & \Delta_k \mathbf{I}_3 \text{ m/s}^3 \end{pmatrix}$
$\Sigma_k^{d,2}$	$2 \cdot 10^{-1} \cdot \frac{\Delta_k^2}{2} \mathbf{I}_4 \text{ s}^{-1}$
$\Sigma_k^{d,3}$	$10 \cdot \Delta_k \mathbf{I}_3 \text{ rad/s}^2$
$\Sigma_k^{d,4}$	$10^{-5} \cdot \begin{pmatrix} \Delta_k \mathbf{I}_3 \text{ m/s}^3 & \mathbf{0} \\ \mathbf{0} & \Delta_k \mathbf{I}_3 \text{ rad/s}^2 \end{pmatrix}$
$\Sigma_k^f$	$8 \cdot 10^{-3} \cdot \mathbf{I}_3 \text{ m/s}^2$
$\Sigma_k^\omega$	$6 \cdot 10^{-3} \cdot \mathbf{I}_3 \text{ rad/s}$

 TABLE II  
 QUANTILES AND MEAN OF ERROR BARS (METERS)

	Smooth movements		Abrupt movements	
	Quartiles	Mean	Quartiles	Mean
4-mix-context-BC	0.09-0.24-0.44	0.32	0.12-0.31-0.65	0.55
3-mix-context-BC	0.09-0.24-0.44	0.32	0.15-0.35-0.73	0.62
2-mix-context-BC	0.09-0.24-0.44	0.32	0.19-0.41-0.85	0.68
ZUPT-EKF	0.31-0.72-1.29	1.01	0.35-0.77-1.74	1.95

Fig. 5 displays the estimated paths with 4-mix-context-BC and ZUPT-EKF implementations, together with the center of the corridors used as performance benchmark. It reveals the flexibility of the proposed techniques in adapting to different pedestrian navigation scenarios especially when compared to conventional approaches, which have difficulty adapting to abrupt sitting and turning actions.

Fig. 6 shows the cumulative error areas over time and the time-slots where the agent stayed seated or still. It manifests the higher drift of conventional approaches in comparison to the proposed framework, and the suitability of additional mixture components to tackle more complex scenarios.

Table II shows the quartile and mean values of the error bars of the proposed techniques against the conventional approach. It also reflects a 68% error reduction for the 2-, 3- and 4-components mixtures under smooth conditions, and a 65%, 68% and 72% error reduction, respectively, under more complex conditions.

## VII. CONCLUSION

The paper established a general framework for context-aided inertial navigation and presented efficient algorithms for its implementation based on BC. The proposed framework provides a principled methodology to merge information from inertial measurements and situational context through Bayesian inference over an augmented HMM. In addition, the developed techniques facilitate accurate learning-based context modeling and efficient data fusion through BC. The experimental results show that the presented algorithms can outperform existing techniques while keeping a processing time in the order of milliseconds. Moreover, the proposed theoretical framework and algorithmic techniques can enable seamless integration of contextual information in inertial navigation systems and significantly improve localization accuracy and robustness.

## APPENDIX A OPERATIONS WITH QUATERNIONS

Let  $\mathbf{p} = [p_0, p_1, p_2, p_3] \in \mathbb{H}$  and  $\mathbf{q} = [q_0, q_1, q_2, q_3] \in \mathbb{H}$  be two quaternions,  $p^s = p_0 \in \mathbb{R}$  and  $q^s = q_0 \in \mathbb{R}$  their respective scalar parts, and  $\mathbf{p}^v = [p_1, p_2, p_3] \in \mathbb{R}^3$  and  $\mathbf{q}^v = [q_1, q_2, q_3] \in \mathbb{R}^3$  their respective vector parts. Their product is defined according to

$$\mathbf{p} \odot \mathbf{q} = \begin{bmatrix} p^s q^s - \mathbf{p}^v \cdot \mathbf{q}^v \\ p^s \mathbf{q}^v + q^s \mathbf{p}^v + \mathbf{p}^v \times \mathbf{q}^v \end{bmatrix}$$

where the dot and cross symbols,  $\cdot$  and  $\times$ , denote the dot and cross product of vectors, respectively. The product of quaternions can likewise be written as a matrix product

$$\mathbf{p} \odot \mathbf{q} = \mathbf{L}(\mathbf{p})\mathbf{q} = \begin{pmatrix} p_0 & -p_1 & -p_2 & -p_3 \\ p_1 & p_0 & -p_3 & p_2 \\ p_2 & p_3 & p_0 & -p_1 \\ p_3 & -p_2 & p_1 & p_0 \end{pmatrix} \begin{bmatrix} q_0 \\ q_1 \\ q_2 \\ q_3 \end{bmatrix}$$

or, equivalently,

$$\mathbf{p} \odot \mathbf{q} = \mathbf{R}(\mathbf{q})\mathbf{p} = \begin{pmatrix} q_0 & -q_1 & -q_2 & -q_3 \\ q_1 & q_0 & q_3 & -q_2 \\ q_2 & -q_3 & q_0 & q_1 \\ q_3 & q_2 & -q_1 & q_0 \end{pmatrix} \begin{bmatrix} p_0 \\ p_1 \\ p_2 \\ p_3 \end{bmatrix}$$

where we have defined the left- and right-multiplication matrices,  $\mathbf{L}(\cdot)$  and  $\mathbf{R}(\cdot)$ , respectively.

The exponential of a quaternion  $\mathbf{q} = [q^s, \mathbf{q}^v] \in \mathbb{H}$  is defined as

$$\exp(\mathbf{q}) = \exp(q^s) \begin{bmatrix} \cos \|\mathbf{q}^v\| \\ \frac{\mathbf{q}^v}{\|\mathbf{q}^v\|} \sin \|\mathbf{q}^v\| \end{bmatrix}.$$

Given a unit quaternion  $\mathbf{q} = [q_0, q_1, q_2, q_3] \in \mathbb{H}$  representing a rotation, the orthogonal matrix

$$\mathbf{C}(\mathbf{q}) = \begin{pmatrix} q_0^2 + q_1^2 - q_2^2 - q_3^2 & 2(q_1 q_2 - q_0 q_3) & 2(q_1 q_3 + q_0 q_2) \\ 2(q_1 q_2 + q_0 q_3) & q_0^2 - q_1^2 + q_2^2 - q_3^2 & 2(q_2 q_3 - q_0 q_1) \\ 2(q_1 q_3 - q_0 q_2) & 2(q_2 q_3 + q_0 q_1) & q_0^2 - q_1^2 - q_2^2 + q_3^2 \end{pmatrix}$$

corresponds to the same rotation.

## APPENDIX B LINEARIZED DYNAMIC MODEL

The nonlinear part of the dynamic model  $f(\mathbf{x}_k | \mathbf{x}_{k-1})$  given by (2), (3) and (4) is

$$\mathbf{q}_k = \mathbf{h}(\mathbf{q}_{k-1}, \boldsymbol{\omega}_{k-1}) = \exp\left(-\frac{\Delta_k}{2} \boldsymbol{\omega}_{k-1}^q\right) \odot \mathbf{q}_{k-1} \quad (18)$$

where  $\boldsymbol{\omega}_{k-1}^q = [0, \boldsymbol{\omega}_{k-1}]$ . Its linearization via first-order Taylor expansion is

$$\mathbf{q}_k = \mathbf{H}_k [[\mathbf{q}_{k-1} - \hat{\mathbf{q}}_{k-1}]^T, [\boldsymbol{\omega}_{k-1} - \hat{\boldsymbol{\omega}}_{k-1}]^T]^T + \mathbf{h}(\hat{\mathbf{q}}_{k-1}, \hat{\boldsymbol{\omega}}_{k-1}) \quad (19)$$

where  $(\hat{\mathbf{q}}_{k-1}, \hat{\boldsymbol{\omega}}_{k-1})$  is the approximation of  $(\mathbf{q}_{k-1}, \boldsymbol{\omega}_{k-1})$  for time step  $k-1$ , and

$$\mathbf{H}_k = \left[ \frac{\partial \mathbf{h}}{\partial \mathbf{q}_{k-1}}(\hat{\mathbf{q}}_{k-1}, \hat{\boldsymbol{\omega}}_{k-1}), \frac{\partial \mathbf{h}}{\partial \boldsymbol{\omega}_{k-1}}(\hat{\mathbf{q}}_{k-1}, \hat{\boldsymbol{\omega}}_{k-1}) \right] \quad (20)$$

is the Jacobian of  $\mathbf{h}$  in (18) evaluated in  $(\hat{\mathbf{q}}_{k-1}, \hat{\boldsymbol{\omega}}_{k-1})$ , with

$$\frac{\partial}{\partial \mathbf{q}_{k-1}} \exp\left(-\frac{\Delta_k}{2} \boldsymbol{\omega}_{k-1}^q\right) \odot \mathbf{q}_{k-1} = \mathbf{L}\left(\exp\left(-\frac{\Delta_k}{2} \boldsymbol{\omega}_{k-1}^q\right)\right) \quad (21)$$

and

$$\begin{aligned} & \frac{\partial}{\partial \boldsymbol{\omega}_{k-1}} \exp\left(-\frac{\Delta_k}{2} \boldsymbol{\omega}_{k-1}^q\right) \odot \mathbf{q}_{k-1} \\ &= -\frac{\Delta_k}{2} \mathbf{R}(\mathbf{q}_{k-1}) \begin{bmatrix} -\frac{\mathbf{r}^T}{\|\mathbf{r}\|} \sin\|\mathbf{r}\| \\ \frac{1}{\|\mathbf{r}\|} \sin\|\mathbf{r}\| \left(\mathbf{I}_3 - \frac{\mathbf{r}\mathbf{r}^T}{\|\mathbf{r}\|^2}\right) + \frac{\mathbf{r}\mathbf{r}^T}{\|\mathbf{r}\|^2} \cos\|\mathbf{r}\| \end{bmatrix} \end{aligned} \quad (22)$$

where  $\mathbf{r} = -\frac{\Delta_k}{2} \boldsymbol{\omega}_{k-1}^q \in \mathbb{R}^3$ , the value for  $\mathbf{r} = \mathbf{0}$  can be obtained as the limit when  $\mathbf{r} \rightarrow \mathbf{0}$ , and the left- and right-multiplication matrices,  $\mathbf{L}(\cdot)$  and  $\mathbf{R}(\cdot)$ , are defined according to Appendix A.

#### ACKNOWLEDGMENT

The authors wish to thank W. Dai, Z. Liu, Y. Shen, B. Teague, and T. Wang for their helpful suggestions and careful reading of the manuscript.

#### REFERENCES

- [1] M. Z. Win, A. Conti, S. Mazuelas, Y. Shen, W. M. Gifford, D. Dardari, and M. Chiani, "Network localization and navigation via cooperation," *IEEE Commun. Mag.*, vol. 49, no. 5, pp. 56–62, May 2011.
- [2] F. Gustafsson and F. Gunnarsson, "Mobile positioning using wireless networks," *IEEE Signal Process. Mag.*, vol. 22, no. 4, pp. 41–53, Jul. 2005.
- [3] Y. Shen, S. Mazuelas, and M. Z. Win, "Network navigation: Theory and interpretation," *IEEE J. Sel. Areas Commun.*, vol. 30, no. 9, pp. 1823–1834, 2012.
- [4] A. Conti, M. Guerra, D. Dardari, N. Decarli, and M. Z. Win, "Network experimentation for cooperative localization," *IEEE J. Sel. Areas Commun.*, vol. 30, no. 2, pp. 467–475, 2012.
- [5] G. Villarrubia, J. F. De Paz, J. Bajo, and J. M. Corchado, "Monitoring and detection platform to prevent anomalous situations in home care," *Sensors*, vol. 14, no. 6, pp. 9900–9921, 2014.
- [6] A. Küpper, *Location-Based Services: Fundamentals and Operation*. Chichester, U.K.: Wiley, 2005.
- [7] Y. Shen and M. Z. Win, "Fundamental limits of wideband localization—Part I: A general framework," *IEEE Trans. Inf. Theory*, vol. 56, no. 10, pp. 4956–4980, Oct. 2010.
- [8] Y. Shen, H. Wymeersch, and M. Z. Win, "Fundamental limits of wideband localization—Part II: Cooperative networks," *IEEE Trans. Inf. Theory*, vol. 56, no. 10, pp. 4981–5000, Oct. 2010.
- [9] F. Zampella, A. Bahillo, J. Prieto, A. R. Jiménez, and F. Seco, "Pedestrian navigation fusing inertial and RSS/TOF measurements with adaptive movement/measurement models: Experimental evaluation and theoretical limits," *Sens. Actuators A, Phys.*, vol. 203, pp. 249–260, 2013.
- [10] D. Dardari, A. Conti, U. Ferner, A. Giorgetti, and M. Z. Win, "Ranging with ultrawide bandwidth signals in multipath environments," *Proc. IEEE*, vol. 97, no. 2, pp. 404–426, Feb. 2009.
- [11] J. Prieto, S. Mazuelas, A. Bahillo, P. Fernández, R. M. Lorenzo, and E. J. Abril, "Adaptive data fusion for wireless localization in harsh environments," *IEEE Trans. Signal Process.*, vol. 60, no. 4, pp. 1585–1596, Apr. 2012.
- [12] U. A. Khan, S. Kar, and J. M. F. Moura, "Distributed sensor localization in random environments using minimal number of anchor nodes," *IEEE Trans. Signal Process.*, vol. 57, no. 5, pp. 2000–2016, 2009.
- [13] J. F. De Paz, D. I. Tapia, R. S. Alonso, C. I. Pinzón, J. Bajo, and J. M. Corchado, "Mitigation of the ground reflection effect in real-time locating systems based on wireless sensor networks by using artificial neural networks," *Knowl. Inf. Syst.*, vol. 34, no. 1, pp. 193–217, 2013.
- [14] J. Prieto, S. Mazuelas, A. Bahillo, P. Fernández, R. M. Lorenzo, and E. J. Abril, "Accurate and robust localization in harsh environments based on V2I communication," in *Vehicular Technologies—Deployment and Applications*. Rijeka, Croatia: Intech, 2013, ch. 7.
- [15] J. Prieto, J. F. De Paz, G. Villarrubia, F. De la Prieta, J. M. Corchado, and F. De la Prieta, "Unified fingerprinting/ranging localization in harsh environments," *Int. J. Distrib. Sens. Netw.*, vol. 2015, no. 3, pp. 1–11, Nov. 2015.
- [16] J. Youssef, "Contributions to pedestrian navigation solutions based on ultra wideband radios, inertial measurement units, and the fusion of both modalities," Ph.D. dissertation, Université Joseph Fourier, Grenoble, France, 2010.
- [17] C. Fischer and H. Gellersen, "Location and navigation support for emergency responders: A survey," *IEEE Pervas. Comput.*, vol. 9, no. 1, pp. 38–47, 2010.
- [18] J. Prieto, S. Mazuelas, A. Bahillo, P. Fernández, R. M. Lorenzo, and E. J. Abril, "Pedestrian navigation in harsh environments using wireless and inertial measurements," in *Proc. 10th Workshop Position. Navigat. Commun. (WPNC)*, Dresden, Germany, Mar. 2013.
- [19] L. Ojeda and J. Borenstein, "Non-GPS navigation for security personnel and first responders," *J. Navigat.*, vol. 60, no. 03, pp. 391–407, Sep. 2007.
- [20] O. J. Woodman, "Pedestrian localisation for indoor environments," Ph.D. dissertation, Univ. of Cambridge, Cambridge, U.K., 2010.
- [21] E. Foxlin, "Pedestrian tracking with shoe-mounted inertial sensors," *IEEE Comput. Graph. Appl.*, vol. 25, no. 6, pp. 38–46, Nov. 2005.
- [22] A. R. Jiménez, F. Seco, J. C. Prieto, and J. I. Guevara, "Indoor pedestrian navigation using an INS/EKF framework for yaw drift reduction and a foot-mounted IMU," in *Proc. 7th Workshop Position. Navigat. Commun. (WPNC)*, Dresden, Germany, Mar. 2010.
- [23] A. R. Jiménez, F. Seco, J. C. Prieto, and J. I. Guevara, "Accurate pedestrian indoor navigation by tightly coupling foot-mounted IMU and RFID measurements," *IEEE Trans. Instrum. Meas.*, vol. 61, no. 1, pp. 178–189, Jan. 2012.
- [24] R. Zhang, F. Hoflinger, and L. Reindl, "Inertial sensor based indoor localization and monitoring system for emergency responders," *IEEE Sensors J.*, vol. 13, no. 2, pp. 838–848, 2013.
- [25] C. Zhou, J. Downey, D. Stancil, and T. Mukherjee, "A low-power shoe-mounted radar for aiding pedestrian inertial navigation," *IEEE Trans. Microw. Theory Tech.*, vol. 58, no. 10, pp. 2521–2528, Oct. 2010.
- [26] C. Zhou, J. Downey, J. Choi, D. Stancil, J. Paramesh, and T. Mukherjee, "A shoe-mounted RF sensor for motion detection," *IEEE Microw. Wireless Compon. Lett.*, vol. 21, no. 3, pp. 169–171, Mar. 2011.
- [27] L. Fang, P. J. Antsaklis, L. A. Montestruque, M. B. McMickell, M. Lemmon, Y. Sun, H. Fang, I. Koutroulis, M. Haenggi, M. Xie, and X. Xie, "Design of a wireless assisted pedestrian dead reckoning system—The NavMote experience," *IEEE Trans. Instrum. Meas.*, vol. 54, no. 6, pp. 2342–2358, Dec. 2005.
- [28] D. H. Titterton and J. L. Weston, *Strapdown Inertial Navigation Technology*, 2nd ed. Stevenage, U.K.: IET, 2004.
- [29] R. Jirawimut, P. Ptasinski, V. Garaj, F. Cecelja, and W. Balachandran, "A method for dead reckoning parameter correction in pedestrian navigation system," *IEEE Trans. Instrum. Meas.*, vol. 52, no. 1, pp. 209–215, 2003.
- [30] J. Hol, T. Schön, H. Luinge, P. Slycke, and F. Gustafsson, "Robust real-time tracking by fusing measurements from inertial and vision sensors," *J. Real-Time Image Process.*, vol. 2, no. 2, pp. 149–160, Nov. 2007.
- [31] B. Krach and P. Robertson, "Integration of foot-mounted inertial sensors into a Bayesian location estimation framework," in *Proc. 5th Workshop Position., Navigat., Commun. (WPNC)*, Hanover, Germany, Mar. 2008.
- [32] P. D. Groves, *Principles of GNSS, Inertial, and Multisensor Integrated Navigation Systems*. Boston, MA, USA: Artech House, 2008.
- [33] U. Walder and T. Bernoulli, "Context-adaptive algorithms to improve indoor positioning with inertial sensors," in *Proc. Int. Conf. Indoor Position. Indoor Navigat. (IPIN)*, Zürich, Switzerland, Nov. 2010.
- [34] M. Ulmke and W. Koch, "Road-map assisted ground moving target tracking," *IEEE Trans. Aerosp. Electron. Syst.*, vol. 42, no. 4, pp. 1264–1274, Oct. 2006.
- [35] S. Mazuelas, Y. Shen, and M. Z. Win, "Belief condensation filtering," *IEEE Trans. Signal Process.*, vol. 61, no. 18, pp. 4403–4415, May 2013.

- [36] Y. Bar-Shalom, X. R. Li, and T. Kirubarajan, *Estimation With Applications to Tracking and Navigation: Theory Algorithms and Software*. New York, NY, USA: Wiley, 2001.
- [37] B. Ristic, S. Arulampalam, and N. Gordon, *Beyond the Kalman Filter. Particle Filters for Tracking Applications*. Boston, MA, USA: Artech House, 2004.
- [38] M. D. Shuster, "A survey of attitude representations," *J. Astronautical Sci.*, vol. 41, no. 4, pp. 439–517, Oct. 1993.
- [39] Y. Wu, "A Critique on "on finite rotations and the noncommutativity rate vector"," *IEEE Trans. Aerosp. Electron. Syst.*, vol. 48, no. 2, pp. 1846–1847, Apr. 2012.
- [40] Y. Wu, H. Zhang, M. Wu, X. Hu, and D. Hu, "Observability of strap-down INS alignment: A global perspective," *IEEE Trans. Aerosp. Electron. Syst.*, vol. 48, no. 1, pp. 78–102, Jan. 2012.
- [41] H. W. Sorenson, *Kalman Filtering: Theory and Application*. Piscataway, NJ, USA: IEEE, 1985.
- [42] S. Julier and J. Uhlmann, "Unscented filtering and nonlinear estimation," *Proc. IEEE*, vol. 92, no. 3, pp. 401–422, Mar. 2004.
- [43] J. A. Richards and X. Jia, "A dempster-shafer approach to context classification," *IEEE Trans. Geosci. Remote Sens.*, vol. 45, no. 5, pp. 1422–1431, May 2007.
- [44] M. Jordan, "Graphical models," *Statist. Sci. Special Issue on Bayesian Statistics*, vol. 19, no. 1, pp. 140–155, 2004.
- [45] M. Rosenblatt, "Remarks on some nonparametric estimates of a density function," *Ann. Math. Statist.*, vol. 27, no. 3, pp. 832–837, Sep. 1956.
- [46] E. Parzen, "On Estimation of a probability density function and mode," *Ann. Math. Statist.*, vol. 33, no. 3, pp. 1065–1076, Sept. 1962.
- [47] J.-N. Hwang, S.-R. Lay, and A. Lippman, "Nonparametric multivariate density estimation: A comparative study," *IEEE Trans. Signal Process.*, vol. 42, no. 10, pp. 2795–2810, Oct. 1994.
- [48] D. W. Scott, *Multivariate Density Estimation*. New York, NY, USA: Wiley, 1992.
- [49] G. McLachlan and D. Pell, *Finite Mixture Models*. Hoboken, NJ, USA: Wiley, 2000.
- [50] F. Daum and J. Huang, "Curse of dimensionality and particle filters," in *Proc. IEEE Aerosp. Conf. IV.*, Mar. 2003, pp. 4\_1979–4\_1993.
- [51] A. H. Stroud and D. Secrest, "Approximate integration formulas for certain spherically symmetric regions," *Math. Comput.*, vol. 17, no. 82, pp. 105–135, 1963.
- [52] P. Hackney, *Making Connections: Total Body Integration Through Bartenieff Fundamentals*. Abingdon, U.K.: Routledge, 2002.
- [53] R. A. Redner and H. F. Walker, "Mixture densities, maximum likelihood and the EM algorithm," *SIAM Rev.*, vol. 26, no. 2, pp. 195–239, 1984.



**Javier Prieto** (S'11–M'12) received his Telecommunication Engineer degree from the University of Valladolid in 2008, his Marketing Research and Techniques degree in 2010, and his Ph.D. in information and communication technologies in 2012.

Since 2015, he is a lecturer and researcher at the University of Salamanca where he is member of the Bioinformatic, Intelligent Systems and Educational Technology (BISITE) group. He was with the Department of Signal Theory of the University of Valladolid where he worked as a lecturer and researcher

in Bayesian inference from 2009 to 2014. In 2014 he was a visiting researcher in the Laboratory for Information Decision Systems (LIDS) at the Massachusetts Institute of Technology (MIT). He previously worked as researcher in a Spanish technological center from 2007 to 2009. His research interests include artificial intelligence for smart cities, localization and navigation for indoor environments, and Bayesian inference for dynamic systems.

Dr. Prieto serves as a guest editor for the *International Journal of Distributed Sensor Networks* and as a reviewer in numerous international journals. He is member of the scientific committee of the *Advances in Distributed Computing and Artificial Intelligence Journal*, and member of several technical program committees including IEEE Globecom in 2014–2015 and IEEE ICC in 2015–2016. In 2013, he received the Extraordinary Performance Award for Doctorate Studies and the "Young entrepreneurs of Castilla y León" award from the Youth Institute of Castilla y León (Spain).



**Santiago Mazuelas** (M'10) received the Ph.D. in mathematics and Ph.D. in telecommunications engineering from the University of Valladolid, Spain, in 2009 and 2011, respectively.

Since 2014 he has been a Staff Engineer at Qualcomm Corporate Research and Development. Prior to joining Qualcomm, he was a Postdoctoral Fellow and Associate in the Laboratory for Information and Decision Systems (LIDS) at the Massachusetts Institute of Technology (MIT) from 2009 to 2014. He previously worked from 2006 to 2009 as a researcher and project manager in a Spanish technological center as well as a junior lecturer in the University of Valladolid. His general research interest is the application of mathematics to solve engineering problems, currently his work is primarily focused on statistical signal processing, machine learning, and data science.

Dr. Mazuelas served as Co-chair for the Symposia on Wireless Communications at the 2014 IEEE Globecom and at the 2015 IEEE ICC. He has been a member of the Technical Program Committee for numerous conferences including the IEEE Globecom in 2010–2015, IEEE ICC in 2013–2015, IEEE VTC in 2012 and 2015, and ICUWB in 2011, and 2013–2015. He has received the Best Student Prize in Telecommunications Technical Engineering from University of Valladolid in 2006, the Best Doctorate Thesis Award from University of Valladolid in 2011, and the Young Scientist Prize from the Union Radio-Scientifique Internationale (URSI) Symposium in 2007. His papers received the IEEE Communications Society Fred W. Ellersick Prize in 2012, and Best Paper Awards from the IEEE ICC in 2013, the IEEE ICUWB in 2011, and the IEEE Globecom in 2011.



**Moe Z. Win** (S'85–M'87–SM'97–F'04) received both the Ph.D. in electrical engineering and the M.S. in applied mathematics as a Presidential Fellow at the University of Southern California (USC) in 1998. He received the M.S. in electrical engineering from USC in 1989 and the B.S. (*magna cum laude*) in electrical engineering from Texas A&M University in 1987.

He is a Professor at the Massachusetts Institute of Technology (MIT) and the founding director of the Wireless Communication and Network Sciences

Laboratory. Prior to joining MIT, he was with AT&T Research Laboratories for five years and with the Jet Propulsion Laboratory for seven years. His research encompasses fundamental theories, algorithm design, and experimentation for a broad range of real-world problems. His current research topics include network localization and navigation, network interference exploitation, intrinsic wireless secrecy, adaptive diversity techniques, and ultra-wideband systems.

Professor Win is an elected Fellow of the AAAS, the IEEE, and the IET, and was an IEEE Distinguished Lecturer. He was honored with two IEEE Technical Field Awards: the IEEE Kiyo Tomiyasu Award (2011) and the IEEE Eric E. Sumner Award (2006, jointly with R. A. Scholtz). Together with students and colleagues, his papers have received numerous awards, including the IEEE Communications Society's Stephen O. Rice Prize (2012), the IEEE Aerospace and Electronic Systems Society's M. Barry Carlton Award (2011), the IEEE Communications Society's Guglielmo Marconi Prize Paper Award (2008), and the IEEE Antennas and Propagation Society's Sergei A. Schelkunoff Transactions Prize Paper Award (2003). Highlights of his international scholarly initiatives are the Copernicus Fellowship (2011), the Royal Academy of Engineering Distinguished Visiting Fellowship (2009), and the Fulbright Fellowship (2004). Other recognitions include the International Prize for Communications Cristoforo Colombo (2013), the Laurea Honoris Causa from the University of Ferrara (2008), the Technical Recognition Award of the IEEE ComSoc Radio Communications Committee (2008), and the U.S. Presidential Early Career Award for Scientists and Engineers (2004).

Dr. Win was an elected Member-at-Large on the IEEE Communications Society Board of Governors (2011–2013). He was the Chair (2004–2006) and Secretary (2002–2004) for the Radio Communications Committee of the IEEE Communications Society. Over the last decade, he has organized and chaired numerous international conferences. He is currently an Editor-at-Large for the IEEE WIRELESS COMMUNICATIONS LETTERS. He served as Editor (2006–2012) for the IEEE TRANSACTIONS ON WIRELESS COMMUNICATIONS, and as Area Editor (2003–2006) and Editor (1998–2006) for the IEEE TRANSACTIONS ON COMMUNICATIONS. He was Guest-Editor for the PROCEEDINGS OF THE IEEE (2009) and for the IEEE JOURNAL ON SELECTED AREAS IN COMMUNICATIONS (2002).